Bioorganic & Medicinal Chemistry 17 (2009) 6942–6951

Contents lists available at ScienceDirect

Bioorganic & Medicinal Chemistry

journal homepage: www.elsevier.com/locate/bmc

New potent P-glycoprotein modulators with the cucurbitane scaffold and their synergistic interaction with doxorubicin on resistant cancer cells

Cátia Ramalhete [a], Joseph Molnár [b], Silva Mulhovo [c], Virgílio E. Rosário [d], Maria-José U. Ferreira [a,*]

[a] iMed.UL, Faculty of Pharmacy, University of Lisbon, Av. das Forças Armadas, 1600-083 Lisbon, Portugal
[b] Department of Medical Microbiology and Immunobiology, University of Szeged, H-6720 Szeged, Hungary
[c] Polytechnic Institute of Gaza (ISPG), Chokwe, Mozambique
[d] CMDT.LA, Institute of Hygiene and Tropical Medicine, UNL, R. da Junqueira 96, 1349-008 Lisbon, Portugal

ARTICLE INFO

Article history:
Received 6 May 2009
Revised 6 August 2009
Accepted 11 August 2009
Available online 15 August 2009

Keywords:
Cucurbitane-type triterpenes
Momordica balsamina
Multidrug resistance
P-glycoprotein MDR modulators
Synergism

ABSTRACT

The novel cucurbitacins, balsaminagenin A and B (**1**–**2**) and balsaminoside A (**3**) and the know cucurbitacin karavelagenin C (**4**), together with five new mono or diacylated derivatives (**5**–**9**) of karavelagenin C were evaluated for multidrug resistance reversing activity on human *MDR1* gene transfected mouse lymphoma cells. Compounds **2**–**6** exhibited a strong activity compared with that of the positive control, verapamil. Structure–activity relationships are discussed. Moreover, in the checkerboard model of combination chemotherapy, the interaction between doxorubicin and compounds **2**–**5** synergistically enhanced the effect of the anticancer drug. Compounds **1**–**4** were isolated from the aerial parts of *Momordica balsamina* L. The structures of the compounds were established on the basis of spectroscopic methods including 2D NMR experiments (COSY, HMQC, HMBC and NOESY).

1. Introduction

The emergence of drug resistance has made many of the currently available anticancer drugs ineffective. Multidrug resistance (MDR) is a kind of acquired drug resistance of cancer cells and microorganisms to a variety of chemotherapeutic agents, which usually are not structurally related. It is a multifactorial phenomenon that can arise through a number of biochemical mechanisms. Although multiple mechanisms can be involved, the most significant mechanism of MDR is that resulting from the overexpression of transporter proteins, such as P-glycoprotein (P-gp), which acts as extrusion pump for chemotherapeutic agents, thereby decreasing their intracellular concentration.[1–3] These proteins belong to the ABC superfamily of transporters that use ATP as energy source. Pgp, characterized by a broad substrate spectrum, which comprises mainly neutral or cationic amphiphilic molecules, is the most important and best-studied ABC transporter.[2,4] The development of compounds (MDR modulators, inhibitors or chemosensitizers) able to restore the cytotoxicity of the available anticancer drugs against MDR tumour cells has been considered among the most realistic approaches to overcome MDR.[5–7] Although a large number of compounds have been found to be able to reverse MDR, so far, no reversal agent has been approved for therapy. Therefore, the discovery of potent and specific P-gp modulators remains a great challenge. In order to achieve this goal, a number of structure–activity relationship (SAR) studies have been carried out. Nevertheless, only general molecular properties have been recognized as important factors, such as the amphiphilic character of the modulators, the presence of aromatic rings, and a positive charge at neutral pH. Hydrophobic and hydrogen bond-acceptor interactions have also been considered important.[8,9] The development of a general and conclusive SAR has been hampered by various limiting factors, mainly the lack of a high-resolution 3D structure of P-gp. Its co-expression with other ABC transporters in MDR tumour cells and its presence in normal tissues has posed a great challenge in the development of agents able to overcome the phenomenon of MDR selectively.[10]

Momordica balsamina L. (Cucurbitaceae), a climber extensively cultivated in many tropical and subtropical regions of the world, is used as food in sub-Saharan Africa.[11] Previous studies on this plant have resulted in the isolation of two phenylpropanoid esters, rosmarinic acid and five pimarane diterpenes.[12,13]

Continuing our efforts to discover effective MDR modulators[14–21] from plants, in this paper we report the isolation from *M. balsamina*, and structure elucidation of three new cucurbitane-type triterpenoids (**1**–**3**), together with one known cucurbitacin (**4**) as well as the preparation of five new (**5**–**9**) acylated derivatives of **4**. These compounds were evaluated for their potential ability as MDR modulators. Furthermore, the antiproliferative effects of the

* Corresponding author. Tel.: +351 21 7946475; fax: +351 21 7946470.
E-mail address: mjuferreira@ff.ul.pt (Maria-José U. Ferreira).

0968-0896/$ - see front matter © 2009 Elsevier Ltd. All rights reserved.
doi:10.1016/j.bmc.2009.08.020

anticancer drug doxorubicin and the most effective modulators, in combination, were studied on human *MDR1* gene transfected mouse lymphoma cells.

2. Results and discussion

2.1. Structure elucidation of compounds

The air-dried powdered aerial parts of *M. balsamina* L. were exhaustively extracted with methanol. Repeated fractionation of the EtOAc soluble part of the methanol extract by column chromatography and further purification by preparative TLC, and HPLC, yielded three new triterpenes with the cucurbitane skeleton (**1**–**3**) and the known cucurbitacin, karavelagenin C (**4**). Karavelagenin C was further derivatized with several acylating reagents (see Section 3), to afford five new cucurbitane-type triterpenes (Fig. 1).

Compound **1**, named balsaminagenin A, was obtained as a white powder with positive optical rotation. The low resolution ESIMS of **1** exhibited pseudomolecular ions at *m/z* 513 $[M+K]^+$, 498 $[M+Na+H]^+$ and 497 $[M+Na]^+$. The molecular formula of **1** was determined as $C_{30}H_{50}O_4$ by ESITOF-HRMS, which showed a pseudomolecular ion at *m/z* 497.3612 (calcd for $C_{30}H_{50}O_4Na$: 497.3601), indicating the presence of six degrees of unsaturation. The IR spectrum of **1** showed a strong absorption band at 3399 cm^{-1}, providing evidence for the presence of hydroxyl groups. The ^1H NMR spectrum exhibited resonances for six tertiary methyl groups (δ 0.76, 0.94, 0.97, 1.05, 2 × 1.25), a secondary methyl group at δ 0.92 (d, J = 5.8 Hz), and two protons attached to oxygenated carbons as broad singlets at δ 3.83 and 3.94, corroborating the presence of the hydroxyl function. Furthermore, signals corresponding to a hydroxymethyl group at δ 3.95 (d, J = 10.8 Hz) and 3.65 (d, J = 10.8 Hz) were also found. In addition, olefinic NMR signals of a trisubstituted double bond at δ 5.74 (d, J = 4.5 Hz) and a disubstituted double bond at δ 5.57 (2H, m) were observed. The above data indicated a tetracyclic triterpene skeleton for **1** carrying a secondary hydroxyl group at C-3. In addition, the marked downfield proton signal of H-3 (δ 3.83) suggested that the hydroxymethyl group was located at C-4 due to oxidation of one of the two geminal methyls at this carbon. Similarly, the downfield resonances of the two geminal methyl groups at δ 1.25 (Me-26, Me-27) indicated that a tertiary hydroxyl group was attached at C-25. The triterpenic nature of **1** was confirmed by combined inspection of ^{13}C NMR and DEPT experiments. These spectra showed 30 carbon resonances corresponding to seven methyl groups, eight methylenes (including an oxygenated at δ_C 69.5), nine methines (two oxygenated at δ_C 68.6 and 75.3, and three sp^2 at δ_C 123.1, 126.0 and 140.8), and six quaternary carbons (one oxygenated carbon at δ_C 71.4, and one olefinic carbon at δ_C 145.2). Analysis of COSY, HMQC and HMBC experiments, coupled with literature data, allowed the unambiguously assignment of all carbon signals (Table 1) of **1**. The HMQC and COSY spectra provided evidence for three important proton spin-systems: $-CH_2-CH(OH)-$ (A); $-CH-C(C)=CH-CH(OH)-CH-$ (B); $-CH_2-CH=CH-$ (C) (Fig. 2). The heteronuclear $^2J_{C-H}$ and $^3J_{C-H}$ connectivities displayed in the HMBC spectrum of **1**, allowed undoubtedly the location of the hydroxyl groups and double bonds. In this way, the long-range correlations observed between C-3 (δ_C 75.3) and the diastereotopic proton signals at δ 3.65 and 3.95 (H-29) and Me-28 (δ 0.97) and between C-29 (δ_C 69.5) and Me-28 and H-3, supported the location of the hydroxyl groups at C-3 and C-29. Similarly, the hydroxyl functions at the allylic positions C-7 and C-25 were further supported by the correlations between the olefinic carbons, C-5 (δ_C 145.2) and C-6 (δ_C 123.1), and the oxymethine H-7 (δ 3.94) and between C-25 and the vinylic protons H-23 and H-24, respectively.

The relative configuration of the tetrahedral stereocenters in the tetracyclic system of **1** was determined through a NOESY experiment (Fig. 3), assuming an α orientation for the angular

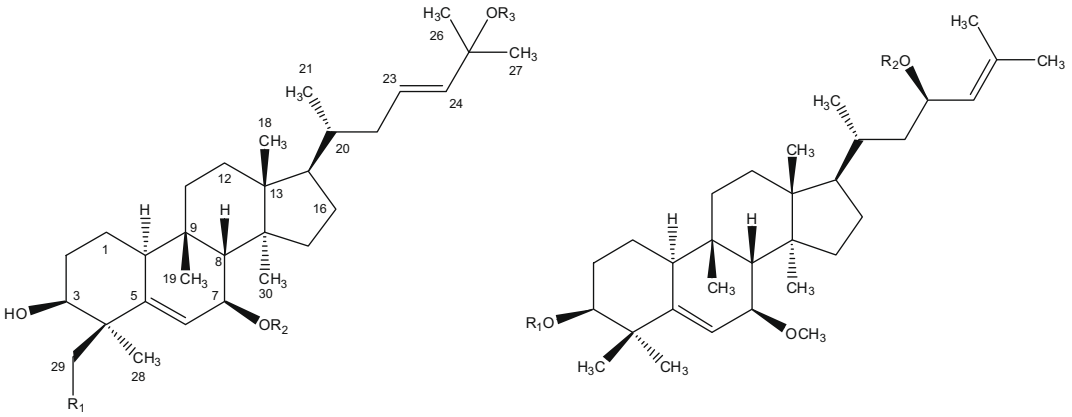

1 R_1 = OH; R_2 = R_3 = H
2 R_1 = OH; R_2 = H; R_3 = CH_3
3 R_1 =H; R_2 = Allose; R_3 = CH_3

4 R_1 = R_2 = H
5 R_1 = H; R_2 = $COCH_3$
6 R_1 = R_2 = $COCH_3$
7 R_1 = H; R_2 =$COCH_2CH_3$
8 R_1 = R_2 = $COCH_2CH_3$
9 R_1 = H; R_2 = $COCH_2CH_2CH_3$

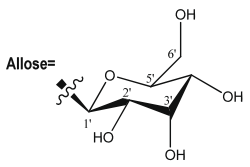

Figure 1. Chemical structures of compounds **1**–**9**.

Table 1
NMR data of compounds **1**–**3**, (MeOD, *J* in Hz)

Position	**1**		**2**		**3**	
	^{1}H	^{13}C	^{1}H	^{13}C	^{1}H[a]	^{13}C[b]
1	1.58 m; 1.70 m	22.0	1.55 m; 1.70 m	22.0	1.57 m; 1.67 m	22.3
2	1.73 m; 1.90 m	30.1	1.70 m; 1.89 m	30.1	1.68 m; 1.97 m	30.1
3	3.83 br s	75.3	3.83 br s	75.3	3.49 br s	77.5
4	–	45.3	–	45.3	–	42.4
5	–	145.2	–	145.1	–	148.7
6	5.74 d (4.5)	123.1	5.74 d (4.7)	123.1	5.75 d (4.9)	122.0
7	3.94 br s	68.6	3.94 br s	68.5	4.11 d (5.0)	74.4
8	1.97 s	53.9	1.98 s	53.9	2.13 s	49.9
9	–	35.0	–	35.0	–	35.1
10	2.32 d (10.2)	39.9	2.32 d (9.2)	39.9	2.33 br d (9.8)	40.1
11	1.48 m; 1.70 m	33.7	1.46 m; 1.70 m	33.7	1.48 m; 1.70 m	33.7
12	1.50 m; 1.68 m	31.3	1.51 m; 1.72 m	31.3	1.49 m; 1.71 m	31.3
13	–	47.1	–	47.1	–	47.2
14	–	49.0	–	49.2	–	49.6
15	1.31 m; 1.38 m	35.7	1.33 m; 1.40 m	35.7	1.38 m	35.7
16	1.38 m; 1.96 m	28.8	1.40 m; 1.95 m	28.8	1.59 m; 1.96 m	28.8
17	1.53 m	51.2	1.53 m	51.2	1.57 m	51.3
18	0.94 s	16.0	0.95 s	16.0	0.98 s	16.1
19	1.05 s	29.7	1.05 s	29.7	1.03 s	29.4
20	1.53 m	37.7	1.54 m	37.6	1.54 m	37.6
21	0.92 d (5.8)	19.2	0.94 d (6.4)	19.3	0.94 d (5.8)	19.3
22	1.76 m; 2.16 d (12.8)	40.3	1.81 m; 2.18 m	40.5	1.82 m; 2.21 m	40.5
23	5.57 m	126.0	5.58 ddd (6.0, 8.8, 15.6)	130.1	5.58 m	130.2
24	5.57 m	140.8	5.38 d (15.6)	137.6	5.38 d (15.7)	137.6
25	–	71.4	–	76.5	–	76.5
26	1.25 s	30.1	1.24 s	26.2	1.24 s	26.2
27	1.25 s	30.0	1.24 s	26.5	1.24 s	26.5
28	0.97 s	23.6	0.97 s	23.6	1.03 s	28.7
29a	3.95 d (10.8)	69.5	3.95 d (10.8)	69.5	1.18 s	26.1
29b	3.65 d (10.8)	–	3.65 d (10.8)	–	–	–
30	0.76 s	18.6	0.75 s	18.6	0.74 s	18.7
25-OMe	–	–	3.13 s	50.6	3.14 s	50.4

[a] ^{1}H NMR signals of 7-allose unit: 4.75 (d, *J* = 7.8 Hz, H-1′), 3.32 (m, H-2′), 4.05 (br s, H-3′), 3.50 (m, H-4′), 3.65 (m, H-6′), 3.84 (d, *J* = 9.8 Hz, H-6′).
[b] ^{13}C NMR signals of 7-allose unit: 99.0 (C-1′), 72.3 (C-2′), 73.0 (C-3′), 69.1 (C-4′), 75.4 (C-5′), 63.2 (C-6′).

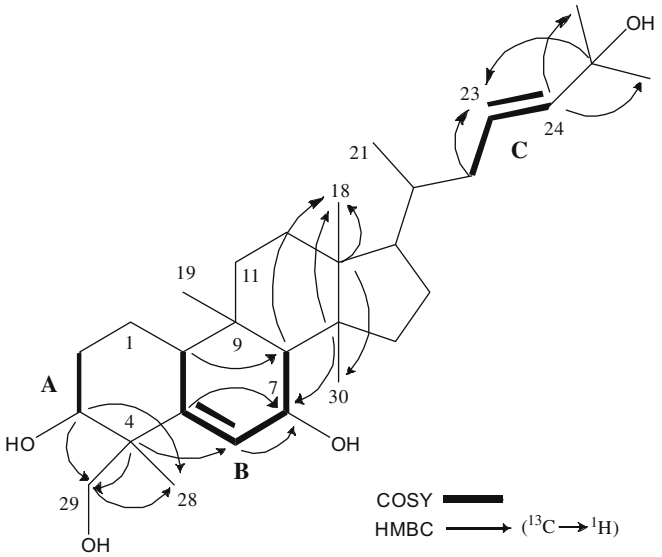

Figure 2. Main ^{1}H–^{1}H COSY and HMBC correlations of compound **1**.

H-10, characteristic of cucurbitacins,[22] and taking in account the coupling constants pattern. The NOE effects observed between H-10α/Me-28, Me-28/H-3, and H-7/Me-30 indicated the β-orientation of the hydroxymethyl at C-4 and the hydroxyl groups at C-7 and C-3. The axial orientation of the hydroxyl group at C-3 was also evidenced by the small coupling constants of H-3, which resonated as a broad singlet, with H-2 protons ($J_{3eq,2ax} \cong J_{3eq,2eq}$). Moreover, nuclear Overhauser interactions were also detected between H-10α/Me-30, Me-30/H-17 and H-17/Me-21, indicating the α configuration of Me-30 and Me-21, usually found in cucurbitane triterpenes. Furthermore, cross-peaks between Me19/H-8 and H-8/Me-18 provided evidence for the β-orientation of these protons. The stereochemistry of the disubstituted double bound at C-23 could not be determined by the *vicinal* coupling constant values of the olefinic signals, due to their overlapping. However, a detailed comparison of the ^{13}C NMR chemical shifts of the side chain carbons of **1**, with those of both *E*/*Z*-isomers of cycloart-23-ene-3β,25-diol,[23] allowed the unequivocally assignment of an *E* geometry to that double bond. From the above data, the structure of **1** was deduced to be cucurbita-5,23(*E*)-diene-3β,7β,25,29-tetraol.

Compound **2**, named balsaminagenin B, was obtained as white needles of mp 110–112 °C and $[\alpha]_D^{20}$ +101 (MeOH, *c* 0.10). Its ESI-TOF-HRMS showed a pseudomolecular ion at *m/z* 511.3758 $[M+Na]^+$ (calcd for $C_{31}H_{52}O_4Na$: 511.3758), indicating a molecular formula of $C_{31}H_{52}O_4$. The ^{13}C and ^{1}H NMR data of compound **2** were very similar to those of compound **1** excepting the signals corresponding to the side chain. When comparing the ^{13}C NMR spectra, compound **2** showed paramagnetic effects at C-23 (+4.1 ppm; γ-carbon) and C-25 (+5.3 ppm; α-carbon) and diamagnetic effects at C-24 (−3.2 ppm; β-carbon), C-26 (−3.6 ppm; β-carbon) and C-27 (−3.5 ppm; β-carbon). Besides, a singlet corresponding to a methoxyl group appeared in the ^{1}H NMR spectrum of **2** at δ 3.13, which showed a ^{13}C resonance at δ_C 50.6. Moreover, in compound **2**, the stereochemistry of the disubstituted double bound at C-23 could be clearly determined as *E* by the large *vicinal* coupling constant values of the olefinic protons signals at δ 5.38 (d, *J* = 15.6 Hz) and δ 5.58 (ddd, *J* = 6.0, 8.8, 15.6 Hz), which

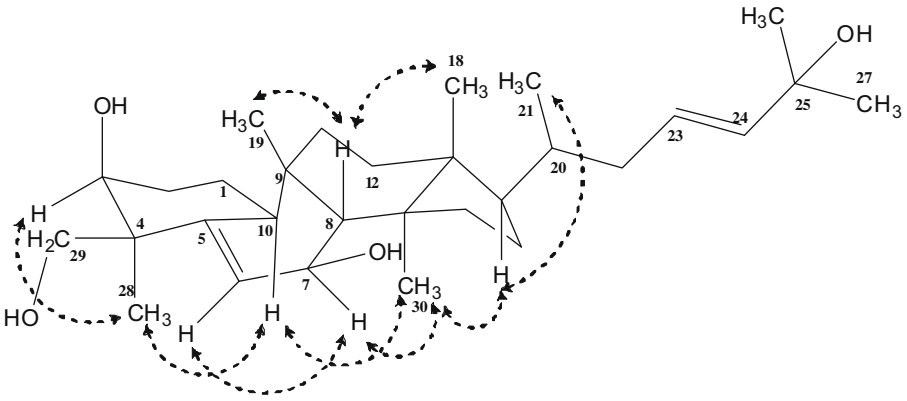

Figure 3. Key NOESY correlations of compound **1**.

were isochronous in compound **1**. The mentioned features indicated that compounds **1** and **2** differ in the substituent at C-25, having compound **2** a methoxyl group at that location instead a hydroxyl group. The position of the methoxyl group was corroborated by the HMBC spectrum, together with COSY and HMQC experiments, which allowed the unambiguous assignment of all the carbon signals of the skeleton (Table 1) and the establishment of the structure of **2** as 25-methoxycucurbita-5,23(*E*)-diene-3β,7β,29-triol.

Although highly oxidized cucurbitacins have been isolated from plants, as far we know, compounds **1** and **2** are the first reported occurrence of related derivatives hydroxylated at C-29.

Compound **3**, named balsaminoside A, was obtained as white crystals, whose molecular formula was determined as $C_{37}H_{62}O_8$ from its ESITOF-HRMS, which showed a pseudomolecular ion at *m/z* 657.4335 $[M+Na]^+$ (calcd for $C_{37}H_{62}O_8Na$: 657.4337). The low resolution ESIMS of **3** exhibited pseudomolecular ions at *m/z* 657 $[M+Na]^+$ and 673 $[M+K]^+$. The fragment ion peaks at *m/z* 478 $[M+Na-C_6H_{11}O_6]^+$ and 203 $[C_6H_{12}O_6+Na]^+$ suggested the presence of a sugar unit. Analysis of the IR spectrum of **3** provided evidence for hydroxyl groups in the molecule (3409 cm^{-1}). Comparison of the ^1H and ^{13}C NMR spectra (Table 1) of **3** with those of compound **2**, revealed six additional signals in the latter, due to the sugar moiety. Furthermore, the signals corresponding to the hydroxymethyl group at C-4 in compound **2** were absent in **3**. Instead, new resonances were observed upfield (δ 1.18; δ_C 26.1), which were ascribed to Me-29. The paramagnetic effects of 2.2, 3.6 and 5.1 ppm at C-3, C-5 and C-28 (γ-carbons), respectively, and the upfield shift of 2.9 ppm at C-4 (β-carbon) observed for compound **3** relatively to **2**, are in agreement with the effects expected for the substitution of an hydroxymethyl by a methyl group. Moreover, in the ^{13}C NMR spectrum of **3**, the signal corresponding to C-7 was shifted downfield ($\Delta\delta_C$ = +5.9), suggesting that the sugar moiety was located at this carbon. The latter was identified, unambiguously, as allose based on the equatorial configuration of H-3′, revealed by a broad singlet at δ_H 4.05. In glucose, H-3′ is axially oriented and generally appears as a triplet ($J_{3ax,2ax} = J_{3ax,4ax}$ = 8.8).[24,25] The identification of the allopyranosyl moiety was corroborated by the values of the carbon signals, which were in good agreement with those reported for allose.[26] The heteronuclear $^3J_{C-H}$ correlations observed in the HMBC spectrum between C-7 (δ_C 74.4) of the aglycone moiety and the anomeric proton (δ 4.75) confirmed that the allopyranosyl unit was bounded at C-7. The relative configuration of **3** was deduced from a NOESY experiment. The configuration of the glycosidic linkage was determined as β based on the coupling constant value of the anomeric proton (J = 7.8 Hz). Therefore, based on the above data, the structure of **3** was assigned as 25-methoxycucurbita-5,23(*E*)-dien-3β-ol-7-*O*-β-D-allopyranoside.

The known cucurbitane-type triterpenoid **4**, was identified as 7β-methoxycucurbita-5,24-diene-3β,23(*R*)-diol by comparison of its IR, MS and NMR spectra with those reported in the literature.[27] The relative stereochemistry of the ring system of **4** was confirmed from a NOESY spectrum. Concerning the side chain, the configuration at C-23, not previously described, was assigned as *R*, by comparison of the ^{13}C NMR data of the side chain carbons of **4** with those reported for the lanostane derivative 23*R*-3-oxolanosta-8,24-dien-23-ol, whose structure was determined by X-ray crystallography, and for a cycloartane derivative with 23*S* configuration.[28,29] In spite of possible free rotation of the side chain, a strong NOE correlation between Me-21 and the oxymethine proton H-23 was found in the NOESY spectrum, suggesting that the side chain has a preferred conformation and, therefore, corroborating the *R* configuration at C-23. This spectroscopic feature was supported by the energy minimization of the 3D structure of compound **4**, which was carried out with the MMFF99x forcefield and a root mean square gradient of 0.00001, using MOE (Molecular Operating Environment).[30] The picture of referred conformation of **4** was made by using PyMOL (see Supplementary data).[31]

Compound **4**, isolated in large amount, was derivatized with several acylating reagents (see Section 3), to afford the following mono esters: 23(*R*)-acetoxy-7β-methoxycucurbita-5,24-dien-3β-ol (**5**), 23(*R*)-propanoyloxy-7β-methoxycucurbita-5,24-dien-3β-ol (7), and 23(*R*)-butanoyloxy-7β-methoxycucurbita-5,24-dien-3β-ol (**9**). The diacylated derivatives 3β,23(*R*)-diacetoxy-7-methoxycucurbita-5,24-diene (**6**) and 3β,23(*R*)-dipropanoyloxy-7-methoxycucurbita-5,24-diene (**8**) were also obtained. The structure elucidation of these new compounds was based on a comparison of their spectroscopic data with those of compound **4**. The main differences were observed for carbon and proton signals of ring A and side chain (Table 2), which were in agreement with the effects expected for acylation of the hydroxyl groups. Analysis of the two-dimensional NMR spectra of compounds **5**–**9** (COSY, HMQC and HMBC), allowed the unambiguously assignment of the carbon signals of their triterpenic skeleton (Table 2).

2.2. Biological activity

Cucurbitacins **1**–**9** were evaluated for their MDR-reversing activities on L15178 mouse T-lymphoma cell line transfected with the human *MDR1* by using the rhodamine-123 exclusion test. P-gp modulating properties were evaluated by comparing the accumulation of rhodamine-123, a specific fluorescent substrate of P-gp, in both MDR-resistant, where P-gp levels are high, and parental cells, as fluorescence activity ratios (FAR). The resulting FAR values are summarized in Table 3. Compounds with FAR values higher than 1 were considered active as P-gp inhibitors and those with FAR values high-

Table 2
^{13}C NMR data for compounds **5**–**9**

C	5[a]	6[a]	7[a]	8[a]	9[b]
1	21.1	21.7	21.1	21.6	21.9
2	28.6	26.4	28.6	26.4	30.0
3	76.8	78.6	76.8	78.4	76.4
4	41.8	39.9	41.7	40.0	42.1
5	146.8	146.8	146.8	146.9	148.1
6	120.9	119.2	120.9	119.2	120.2
7	77.2	77.3	77.2	77.3	77.9
8	47.9	47.7	47.9	48.0	49.3
9	34.0	34.0	34.0	34.0	34.8
10	38.7	38.7	38.7	38.6	39.7
11	32.6	32.4	32.6	32.4	33.6
12	30.1	30.1	30.1	30.1	31.0
13	46.2	46.1	46.2	46.2	46.9
14	47.9	47.9	47.9	48.0	48.8
15	34.6	34.6	34.6	34.6	35.4
16	27.8	27.8	27.8	27.8	28.6
17	50.5	50.5	50.5	50.5	51.3
18	15.3	15.3	15.3	15.3	15.7
19	28.8	28.5	28.8	28.5	29.3
20	32.8	32.8	32.8	32.8	33.4
21	19.0	18.9	19.0	19.0	19.3
22	42.0	41.9	42.0	42.0	42.8
23	69.5	69.4	69.3	69.3	69.1
24	124.7	124.7	124.7	124.7	126.0
25	135.7	135.7	135.6	135.6	135.7
26	18.4	18.3	18.3	18.3	18.5
27	25.7	25.7	25.7	25.7	26.1
28	27.9	28.0	27.8	28.0	28.5
29	25.4	24.8	25.4	24.9	25.7
30	18.0	17.9	18.0	17.9	18.4
7-OCH$_3$	56.3	56.3	56.3	56.3	56.2
1′	170.7	170.6	174.0	174.0[c]	173.0
2′	21.4	21.4	28.0	28.0	19.3
3′	—	—	9.3	9.3[d]	36.9
4′	—	—	—	—	13.9
1″	—	170.9	—	174.2[c]	—
2″	—	21.3	—	28.0	—
3″	—	—	—	9.4[d]	—

[a] In $CDCl_3$.
[b] In CD_3COCD_3.
[c,d] Interchangeable assignments.

er than 10 strong MDR modulators.[32] Verapamil, a well-known chemosensitizer, was applied as a positive control. Two concentrations (2 and 20 μM) were used in the experiments. Compound **4** was also studied at 0.5 and 1 μM concentration (Table 3).

The antiproliferative effects of the compounds were also assessed on the above referred cells. Results are summarized in Table 4. As can be observed, in the MDR subline, the compounds showed no significant toxic effect or a week activity at a concentration similar or higher than the highest concentration used in the MDR reversal experiments. Besides, it should be emphasized that cytotoxicity and MDR reversal activity can not be directly compared. In fact, MDR assay is a short term experiment (30 min) where a large number of cells (10,000) were treated with the compounds while in the cytotoxicity assay a few thousands of cells were treated with the compounds for 72 h.

At the highest concentration all compounds, excepting compound **8**, were found to be strong P-gp inhibitors (fluorescence activity ratio FAR = 20.0–104.2 at 20 μM concentration), exhibiting balsaminagenin B (**2**) (FAR = 5.98 and 104.2 at 2 and 20 μM, respectively) and balsaminoside A (**3**) (FAR = 1.45 and 89.4 at 2 and 20 μM, respectively) the highest effects, and a manifold activity when compared to that of the positive control verapamil (FAR = 7.4–8.6 at 22 μM concentration). However, compounds **1**, **8** and **9** were found to be inactive at the concentration of 2 μM. At this concentration, compounds **4** (FAR = 42.1 and 46.0 at 2 and 20 μM, respectively) and **5** (FAR = 35.2 and 34.2 at 2 and 20 μM, respectively) exhibited the highest effect in reversing MDR. Nevertheless, for both compounds, this concentration was at the saturation zone. In fact, when compound **4** was assayed at 0.5 and 1 μM a dose-dependent effect was observed, with a very significant activity at the highest concentration applied (FAR = 1.5 and 15.0 at 0.5 and 1 μM, respectively).

In order to find out structure–activity relationships, theoretical octanol/water partition coefficients and other physico-chemical properties were calculated (Table 5). As can be observed in Table 5, all compounds are lipophilic, exhibiting log *P* values in the range of 5.2–8.6. They have a molecular weight comprised between 634 and 472 and are H-bond acceptors (between 3 and 8). Excluding compounds **6** and **8**, they are also H-bond donors (between 1 and 5). It is interesting to note that karavelagenin C (**4**), the most active compound at the lowest concentration, has the lowest values of topological polar surface area (49.7) and molecular weight (472). However, the correlation between the MDR reversing effects and

Table 3
Effect of compounds (**1**–**9**) on reversal of multidrug resistance (MDR) on human *MDR1* gene-transfected mouse lymphoma cells

Compound	Concentration (μM)	FSC[a]	SSC[a]	FL-1[a]	FAR
PAR + R123[b]	—	464.7	195.7	974.2	
MDR + R123[c]	—	468.8	247.0	25.6	
Verapamil	22.0	439.2	251.1	154.5	8.6
1[d]	2.0	441.8	261.2	13.95	1.07
	20.0	447.4	257.6	579.8	44.3
2[d]	2.0	428.7	261.1	78.4	5.98
	20.0	454.4	238.6	1365.1	104.2
3[d]	2.0	429.6	253.8	19.0	1.45
	20.0	441.6	249.7	1171.1	89.4
4[d]	0.5	456.4	215.3	12.7	1.5
	1.0	460.7	217.8	130.0	15.0
	2.0	468.8	215.4	365.7	42.1
	20.0	551.8	206.8	399.5	46.0
5	2.0	470.2	254.9	671.2	35.2
	20.0	518.1	222.4	612.7	34.2
6	2.0	454.9	247.0	102.1	5.7
	20.0	462.9	249.3	671.2	37.5
7	2.0	466.3	249.9	30.3	1.7
	20.0	481.3	242.5	726.8	40.6
8	2.0	454.0	237.9	16.2	0.9
	20.0	463.1	230.8	42.3	2.4
9	2.0	448.7	235.9	18.0	1.0
	20.0	461.9	236.3	388.7	21.7
DMSO	10 μL	441.76	237.54	13.75	0.8

[a] FSC: Forward scatter count of cells in the samples (cell size ratio); SSC: Side scatter count of cells in the samples; FL-1: Mean fluorescence intensity of the cells. FAR: fluorescence activity ratio: values were calculated by using the equation given in Section 3.
[b] PAR control: a parental cell without MDR gene.
[c] MDR: a parental cell line transfected with human *MDR1* gene.
[d] The results of compounds **1**–**3** (PAR + R123: FL-1 = 959.5; MDR + R123: FL-1 = 10.6; verapamil: FL-1 = 97.1; FAR = 7.4), and **4** (PAR + R123: FL-1 = 1034.3; MDR + R123: FL-1 = 9.5; verapamil: FL-1 = 73.7; FAR = 8.5) were obtained from different assays.

Table 4
Antiproliferative effects of compounds **1**–**9** on parental (PAR) and multidrug resistance (MDR) mouse lymphoma cell lines (L5178)

Compound	PAR[a] ID_{50} (μM)	MDR[a] ID_{50} (μM)
1	19.5 ± 0.7	25.9 ± 2.4
2	15.4 ± 2.4	16.8 ± 1.9
3	8.3 ± 1.9	20.8 ± 1.7
4	6.3 ± 1.5	16.8 ± 2.2
5	26.0 ± 4.3	34.8 ± 3.6
6	48.8 ± 2.4	60.2 ± 5.6
7	41.4 ± 4.6	43.5 ± 2.0
8	>133.3	>133.3
9	51.0 ± 7.2	73.8 ± 2.1

[a] Values represent the mean ± SD of three independent experiments.

calculated physico-chemical properties must be multifactorial because none of the calculated parameters were directly correlated alone. When comparing FAR values of compound **4** and its acylated derivatives, it may be considered that the free hydroxyl groups at both C-3 and C-23 are crucial for the activity. In fact, compound **4**, which bears a free allylic hydroxyl group at C-23, showed a higher activity than its corresponding monoacylated derivatives **5**, **7** and **9** (FAR = 35.2, 1.7 and 1.0, respectively at 2 μM); furthermore, as can be deduced by the drastic decrease observed in FAR values obtained for propanoyl (**7**) and butyril (**9**) monoesters, MDR reversal activity was also affected by the number of carbons of the acylating agent, highlighting the involvement of other factors in the activity, besides lipophilicity. When considering the acylation at C-3 in the diacylated derivatives **6** and **8** (FAR = 5.7, 0.9, respectively at 2 μM) the decrease of the activity, previously observed in the corresponding monoesters (**5** and **7**), is accentuated.

Compounds **1**–**3**, differ from compounds **4**–**9**, having a double at C-23, instead of a hydroxyl function and a hydroxyl/methoxyl group at C-25. Besides, ring A bears an extra hydroxyl group at C-29. Compound **2** was the most active, exhibiting a very high fluorescence activity ratios at the highest concentration (FAR = 104.2 at 20 μM). The methoxyl group at C-25 appears to play an important role being responsible for the higher activity of compound **2** when compared to that of **1**. The substitution of the hydroxyl at C-7 by the sugar moiety in compound **3**, which has the highest topological polar surface area (TSPA = 128.8), decreased the activity.

In further experiments, some of the most effective resistance modulators (**2**–**5**) were studied in combination with doxorubicin, on human *MDR1* gene-transfected mouse lymphoma cells, using the checkerboard microplate method. Several concentrations of doxorubicin and resistance modifiers were tested. Figures 4 and 5 reveal that all these compounds exhibited a synergistic effect with doxorubicin on the studied cell line (Table 6). The most effective compound was balsaminagenin B (**2**), which expressed a significant synergy in checkerboard experiments having a fractional inhibitory index of 0.18.

3. Experimental section

3.1. General experimental procedures

Melting points were determined on a Köfler apparatus and are uncorrected. Optical rotations were obtained using a Perkin Elmer 241 polarimeter. IR spectra were determined on a FTIR Nicolet Impact 400, and NMR spectra recorded on a Bruker ARX-400 NMR spectrometer (^{1}H 400 MHz; ^{13}C 100.61 MHz), using MeOD, $CDCl_3$ and acetone as solvents. ESIMS were taken on a Micromass® Quattro micro™ API and ESITOF-HRMS on a Bruker-Microtof ESI-TOF. TLC was performed on precoated SiO_2 F_{254} plates (Merck 5554 and 5744), with visualization under UV light and by spraying with sulfuric acid–methanol (1:1), followed by heating. Column chromatography (CC) was carried out on silica gel (Merck 9385). TLC were performed on precoated silica gel F_{254} plates (Merck 5554 and 5744) and visualized under UV light and by spraying sulfuric acid–methanol (1:1) followed by heating. HPLC was carried out on a Merck-Hitachi instrument, with UV detection (210 nm), using a Merck LiChrospher 100 RP-18 (10 μm, 250 × 10 mm) column.

Table 5
Physico-chemical properties (number of hydrogen bond acceptors and donors, molecular weight, topological polar surface area and octanol/water partition coefficient)[a] of compounds (**1**–**9**)

Compound	No. H		MW	TSPA	log *P*
	Acceptors	Donors			
1	4	4	474	80.9	5.2
2	4	3	488	69.9	5.8
3	8	5	634	128.8	5.3
4	3	2	472	49.7	7.3
5	4	1	514	55.8	8.0
6	5	0	556	61.8	8.6
7	4	1	528	55.8	8.3
8	5	0	584	61.8	8.9
9	4	1	542	55.8	8.7

[a] Physico-chemical parameters were determined by using the JME molecular editor (version April 2009, http://www.molinspiration.com/).

3.2. Plant material

The aerial parts of *M. balsamina* were collected in Gaza, Mozambique, in August 2006. The plant Material was identified by Dr. Silva Mulhovo, and a voucher specimen (30 SM) has been deposited at the herbarium (LMA) of Instituto de Investigação Agronómica of Mozambique.

3.3. Compounds studied

3.3.1. Extraction and isolation

The air-dried aerial parts of *M. balsamina* L. (1.2 kg) were mechanically powdered and exhaustively extracted with methanol (11 × 8 L), at room temperature. Evaporation of the solvent (under *vacuum*, 40 °C) from the crude extract yielded a residue (280 g), which was suspended in H_2O (1 L) and extracted with EtOAc (9 × 0.5 L). The residue (85 g) of the EtOAc extract was suspended in MeOH/H_2O (9:1; 1 L), and extracted with *n*-hexane (5 × 0.5 L) for removal of waxy material that was not further studied. The remaining extract was dried (Na_2SO_4) and evaporated under *vacuum* (40 °C), yielding a residue (45 g) that was chromatographed over SiO_2 (1 kg), using mixtures of *n*-hexane/EtOAc (1:0 to 0:1) and EtOAc/MeOH (19:1 to 0:1) as eluents. According to differences in composition, as indicated by TLC, six crude fractions were obtained (Fr 1–6). Fr 2 crystallized during the elution procedure (*n*-hexane/EtOAc, 1:1) yielding 840 mg of compound **4**. Fr 4 (3.25 g), eluted with mixtures of *n*-hexane/EtOAc (1:19 to 0:1), was subjected to a silica gel column chromatography with mixtures of increasing polarity of *n*-hexane/EtOAc (4:1 to 0:1) and EtOAc/MeOH (1:0 to 1:1) to give seven fractions. The subfraction 4_5 (1.27 g) eluted with EtOAc/MeOH (1:0 to 9:1) was successively rechromatographed by column chromatography, using mixtures of CH_2Cl_2/MeOH (1:0 to 0:1) and further purified by preparative TLC ($CHCl_3$/MeOH, 9:1), to give 16 mg of compound **2**. Fr 5 (2.8 g), eluted with mixtures of EtOAc/MeOH (99:1 to 93:7), was chromatographed on SiO_2 with mixtures of *n*-hexane/EtOAc (1:1 to 0:1) and EtOAc/MeOH (49:1 to 0:1), giving four fractions. The fraction eluted with *n*-hexane/EtOAc (3:17 to 1:19) was successively chromatographed over SiO_2 with mixtures of CH_2Cl_2/MeOH of increasing polarity. A final purification by HPLC yielded 15 mg of compound **1** (MeOH/H_2O 3:1, 5 mL/min, t_R = 30 min).

Compound **3** (49 mg) was obtained from the crude fraction Fr 6, eluted with a mixture of EtOAc/MeOH (9:1) after successive column chromatography and further purification by HPLC (MeOH/H_2O 4:1, 5 mL/min, t_R = 33 min).

3.3.1.1. Cucurbita-5,23(*E*)-diene-3β,7β,25,29-tetraol (1). Amorphous, white powder; $[\alpha]_D^{20}$ +86 (*c* 0.11, MeOH); IR (KBr) ν_{max} 3399, 2934, 1651, 1457, 1404, 1154, 1054 cm^{-1}; ^{1}H and ^{13}C NMR data, see Table 1; ESIMS *m/z* (rel. int.): 513 $[M+K]^+$ (11), 498 $[M+Na+H]^+$ (24), 497 $[M+Na]^+$ (66). ESITOF-HRMS *m/z*: 497.3612 (calcd for $C_{30}H_{50}O_4Na$ $[M+Na]^+$, 497.3601).

3.3.1.2. 25-Methoxycucurbita-5,23(*E*)-diene-3β,7β,29-triol (2). White needles; mp 110–112 °C; $[\alpha]_D^{20}$ +101 (*c* 0.1, MeOH); IR (KBr) ν_{max} 3409, 2941, 1402, 1075 cm^{-1}; ^{1}H and ^{13}C NMR data,

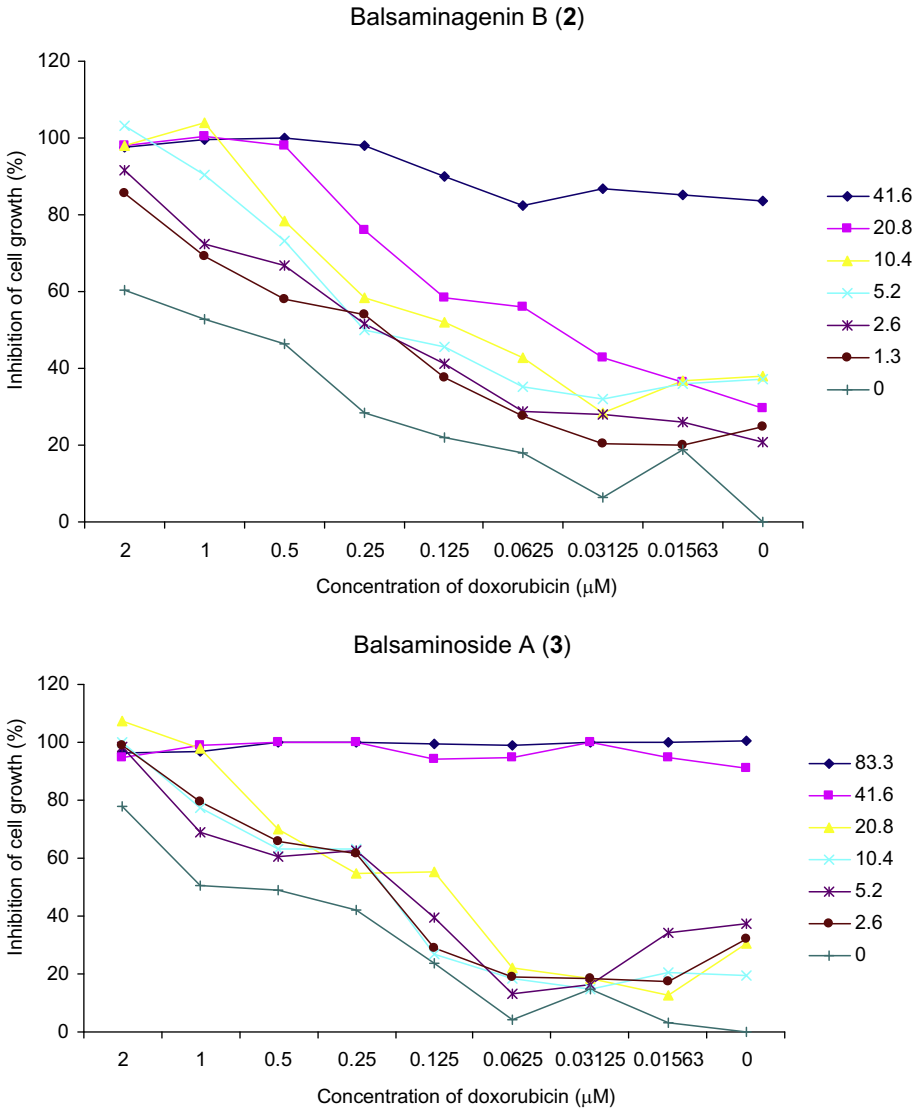

Figure 4. Effect of balsaminagenin B (**2**) (41.5–0 μM), and balsaminoside A (**3**) (83.3–0 μM) in combination with doxorubicin on L5178 cell line.

see Table 1; ESIMS *m/z* (rel. int.): 511 $[M+Na]^+$ (100). ESITOF-HRMS *m/z*: 511.3758 (calcd for $C_{31}H_{52}O_4Na$ $[M+Na]^+$, 511.3758).

3.3.1.3. 25-Methoxycucurbita-5,23(*E*)-dien-3β-ol-7-*O*-β-D-allopyranoside (3). White crystals; mp 220 °C; $[\alpha]_D^{20}$ +69 (*c* 0.1, MeOH); IR (KBr) ν_{max} 3409, 2928, 1456, 1375, 1068 cm^{-1}; ^1H and ^{13}C NMR data in MeOD, see Table 1; ^1H NMR (400 MHz, C_5D_5N): 6.09 (d, *J* = 4.96 Hz, H-24), 5.64 (m, H-23), 5.59 (d, *J* = 7.56 Hz, H-1′), 5.58 (d, *J* = 15.92 Hz, H-24), 4.79 (br s, H-3′), 4.60 (m, H-7/H-6′), 4.53 (m, H-5′), 4.48 (m, H-6′), 4.32 (br s, H-4′), 4.07 (br s, H-2′), 3.82 (br s, H-3), 3.23 (s, 25-OCH_3), 2.46 (s, H-8), 2.40 (m, H-10), 1.46 (s, H-28), 1.40 (s, H-19), 1.34 (s, H-26/H-27), 1.14 (s, H-29), 0.98 (d, *J* = 4.8 Hz, H-21), 0.82 (s, H-18), 0.73 (s, H-30). ^{13}C NMR (100.61 MHz, C_5D_5N): 148.2 (C-5), 137.6 (C-24), 128.5 (C-23), 121.2 (C-6), 98.3 (C-1′), 76.1 (C-5′), 76.0 (C-3), 74.8 (C-25), 73.2 (C-3′), 72.4 (C-2′), 72.0 (C-7), 69.3 (C-4′), 63.3 (C-6′), 50.3 (C-17), 50.1 (OCH_3), 48.4 (C-14), 48.2 (C-8), 46.2 (C-13), 41.9 (C-4), 39.7 (C-22), 39.2 (C-10), 36.4 (C-20), 34.8 (C-15), 34.4 (C-9), 32.9 (C-12), 30.4 (C-16), 30.1 (C-2), 29.3 (C-19), 28.4 (C-11), 27.8 (C-29), 26.4 (C-27), 26.0 (C-26/C-28), 21.7 (C-1), 19.0 (C-21), 18.0 (C-30), 15.6 (C-18). ESIMS *m/z* (rel. int.): 657 $[M+Na]^+$ (100), 673 $[M+K]^+$ (2), 478 $[M+Na-C_6H_{11}O_6]^+$ (1), 203 $[C_6H_{12}O_6+Na]^+$ (13). ESITOF-HRMS *m/z*: 657.4335 (calcd for $C_{37}H_{62}O_8Na$ $[M+Na]^+$, 657.4337).

3.3.2. Acylation of 7β-methoxycucurbita-5,24-diene-3β,23(*R*)-diol

7β-Methoxycucurbita-5,24-diene-3β,23(*R*)-diol was derivatized with several acylating reagents as described below, to afford five new cucurbitane derivatives (**5**–**9**).

3.3.2.1. Acetylation with acetic anhydride. Compound **4** (42.5 mg) was treated with a mixture of acetic anhydride (1 mL) and pyridine (1 mL), and the mixture was stirred at room temperature for 1 h. The excess of pyridine and acetic anhydride were removed with N_2. The residue was purified by chromatography using mixtures of *n*-hexane/EtOAc (1:0 to 4:1) as eluents to give compounds **5** (11.4 mg) and **6** (31.7 mg).

23(R)-Acetoxy-7β-methoxycucurbita-5,24-dien-3β-ol **5**: colorless oil; ESIMS *m/z* (rel. int.): 578 $[M+Na+ACN]^+$ (100), 537 $[M+Na+ACN]^+$ (18), 477 $[M+Na-OCOCH_3]^+$ (5). ^1H NMR (400 MHz, $CDCl_3$) δ 5.85 (d, *J* = 4.9 Hz, H-6), 5.60 (td, *J* = 2.7, 9.8 Hz, H-23), 5.11 (d, *J* = 8.7 Hz, H-24), 3.53 (br s, H-3), 3.44 (d, *J* = 4.8 Hz, H-7), 3.36 (s, OCH_3), 2.29 (d, *J* = 8.5 Hz, H-10), 2.06 (s,

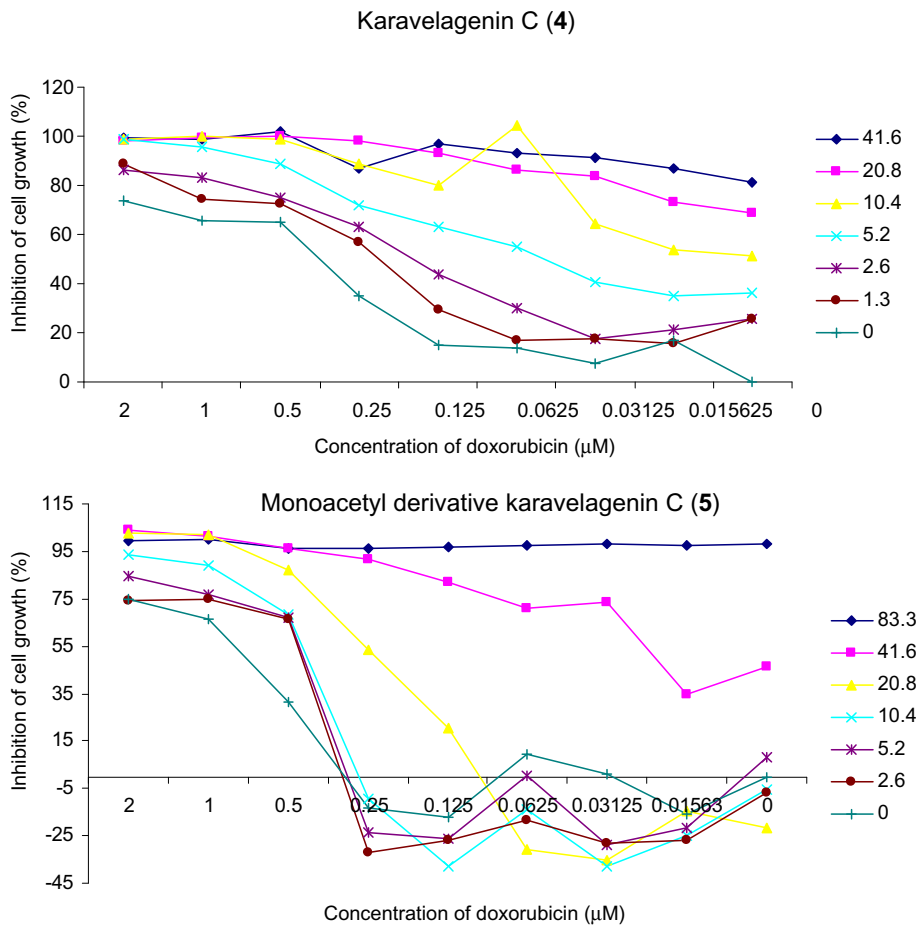

Figure 5. Effect of karavelagenin C (**4**) (41.5–0 μM) and its monoacetyl derivative (**5**) (83.3–0 μM) in combination with doxorubicin on L5178 MDR cell line.

Table 6
In vitro effects of compounds **2**–**5** in combination with doxorubicin on human *MDR1* gene-transfected mouse lymphoma cell line

Compounds	FIX value[a]	Interaction
2	0.18	Synergism
3	0.37	Synergism
4	0.28	Synergism
5	0.44	Synergism

[a] FIX: fractional inhibitory index.

H-8), 2.04 (s, H-2′), 1.74 (s, H-27), 1.71 (s, H-26), 1.22 (s, H-29), 1.05 (s, H-28), 1.00 (s, H-19), 0.96 (d, J = 5.5 Hz, H-21), 0.93 (s, H-18), 0.71 (s, H-30).

3β,23(R)-Diacetoxy-7-methoxycucurbita-5,24-diene **6**: colorless oil; ESIMS *m/z* (rel. int.): 579 $[M+Na]^+$ (31), 620 $[M+Na+ACN]^+$ (17), 519 $[M+Na-OCOCH_3]^+$ (4). ^1H NMR (400 MHz, $CDCl_3$) δ 5.77 (d, J = 4.9 Hz, H-6), 5.60 (td, J = 2.7, 9.8 Hz, H-23), 5.09 (d, J = 8.8 Hz, H-24), 4.74 (br s, H-3), 3.42 (d, J = 5.0 Hz, H-7), 3.35 (s, OCH_3), 2.27 (d, J = 10.7 Hz, H-10), 2.04 (s, H-8), 2.01 (s, H-2′), 1.99 (s, H-2″), 1.72 (s, H-27), 1.69 (s, H-26), 1.10 (s, H-29), 1.06 (s, H-28), 0.97 (s, H-19), 0.94 (d, J = 5.5 Hz, H-21), 0.91 (s, H-18), 0.70 (s, H-30).

3.3.2.2. Acylation with propionic anhydride. To compound **4** (56 mg) was added pyridine (1 mL) and propionic anhydride (1 mL), and the mixture was stirred at room temperature for eight hours. The reaction mixture was poured into ice-water and extracted with CH_2Cl_2. The combined organic layers were washed sequentially with a solution of HCl (1%) followed by a solution of Na_2CO_3 (4%). The product obtained was purified by preparative TLC ($CHCl_3$/MeOH; 19:1) to afford compounds **7** (28.0 mg) and **8** (11.0 mg).

23(R)-Propanoyloxy-7β-methoxycucurbita-5,24-dien-3β-ol **7**: colorless oil; ESIMS *m/z* (rel. int.): 552 $[M+H+Na]^+$ (79), 478 $[M+H-OCOCH_2CH_3]^+$ (100). ^1H NMR (400 MHz, $CDCl_3$) δ 5.85 (d, J = 5.1 Hz, H-6), 5.63 (td, J = 2.9, 9.9 Hz, H-23), 5.10 (d, J = 8.2 Hz, H-24), 3.53 (br s, H-3), 3.44 (d, J = 5.3 Hz, H-7), 3.36 (s, OCH_3), 2.31 (m, H-10/H-2′), 2.06 (s, H-8), 1.75 (s, H-27), 1.71 (s, H-26), 1.22 (s, H-29), 1.15 (t, J = 7.5 Hz, H-3′), 1.05 (s, H-28), 1.00 (s, H-19), 0.96 (d, J = 5.2 Hz, H-21), 0.92 (s, H-18), 0.71 (s, H-30).

3β,23(R)-Dipropanoyloxy-7β-methoxycucurbita-5,24-diene **8**: colorless oil; ESIMS *m/z* (rel. int.): 608 $[M+H+Na]^+$ (11), 534 $[M+H-OCOCH_2CH_3]^+$ (15). ^1H NMR (400 MHz, $CDCl_3$) δ 5.79 (d, J = 4.4 Hz, H-6), 5.63 (td, J = 2.9, 9.9 Hz, H-23), 5.11 (d, J = 8.8 Hz, H-24), 4.77 (br s, H-3), 3.45 (d, J = 4.4 Hz, H-7), 3.37 (s, OCH_3), 2.35–2.25 (m, H-10/H-2′/H-2″), 2.06 (s, H-8), 1.76 (s, H-27), 1.71 (s, H-26), 1.13 (m, H-3′/H-3″), 1.10 (s, H-29), 1.08 (s, H-28), 0.99 (s, H-19), 0.96 (d, J = 5.6 Hz, H-21), 0.93 (s, H-18), 0.73 (s, H-30).

3.3.2.3. Acylation with butyric anhydride. Compound **4** (30 mg) was suspended in butyric anhydride (0.5 mL) and pyridine (0.5 mL). After stirring at room temperature for 72 h, the excess of pyridine was eliminated with N_2 and the residue was purified by chromatography, using mixtures of *n*-hexane/EtOAc (13:7 to 1:1), followed by preparative TLC (*n*-hexane/EtOAc; 3:2), to afford compound **9** (15 mg).

23(R)-Butanoyloxy-7β-methoxycucurbita-5,24-dien-3β-ol **9**: colorless oil. ESIMS *m/z* (rel. int.): 607 $[M+Na+ACN]^+$ (49), 565 $[M+Na]^+$ (19), 581 $[M+K]^+$ (11), 477 $[M+H-OCOCH_2CH_2CH_3]^+$ (9). ^1H NMR (400 MHz, CD_3COCD_3) δ 5.77 (d, J = 4.5 Hz, H-6), 2.67 (td, J = 2.9, 10.4 Hz, H-23), 5.13 (d, J = 8.9 Hz, H-24), 3.50 (br s, H-3), 3.40 (d, J = 4.4 Hz, H-7), 3.31 (s, OCH_3), 2.35 (d, J = 10.3 Hz, H-10), 2.24 (t, J = 7.3 Hz, H-2′), 1.72 (s, H-26), 1.69 (s, H-27), 1.62 (m, H-3′), 1.19 (s, H-29), 1.03 (s, H-28), 0.98 (d, J = 5.8, H-21), 0.96 (s, H-19), 0.94 (s, H-18), 0.92 (t, J = 7.4 Hz, H-4′), 0.77 (s, H-30).

3.4. Biological assays

3.4.1. Cell cultures

L5178 mouse T-cell lymphoma cells were transfected with pHa *MDR1*/A retrovirus, as previously described.[33] *MDR1*-expressing cell lines were selected by culturing the MKJinfected cells with 60 ng/mL colchicine to maintain the expression of the MDR phenotype in all cells of the population. L5178 (parent) mouse T-cell lymphoma cells and the human *MDR1*-transfected subline were cultured in Mccoy's 5A medium supplemented with 10% heat-inactivated horse serum, L-glutamine and antibiotics. This cell line was cultured at 37 °C, and maintained in a 5% CO_2 atmosphere.

3.4.2. Assay for antiproliferative effect

The effects of increasing concentrations of the drugs alone on cell growth were tested in 96-well flat-bottomed microtitre plates. The compounds were diluted in a volume of 50 μL medium. Then, 1×10^4 cells in 0.1 mL of medium were added to each well, with the exception of the medium controll wells. The culture plates were further incubated at 37 °C for 72 h; at the end of the incubation period, 15 μL of MTT (thiazoil blue, Sigma, St. Louis, MO, USA) solution (from a 5 mg/mL stock) was added to each well. After incubation at 37 °C for 4 h, 100 μL of sodium dodecyl sulfate (SDS) (Sigma) solution (10%) was measured into each well and the plates were further incubated at 37 °C overnight. The cell growth was determined by measuring the optical density (OD) at 550 nm (ref. 630 nm) with the Dynatec MRX vertical beam ELISA reader. Inhibition of the cell growth was determined according to the formula:

$$100 - \left[\frac{\text{OD sample} - \text{OD medium control}}{\text{OD cell control} - \text{OD medium control}}\right] \times 100$$

The ID_{50} values are expressed as means ± SD from three experiments.

3.4.3. Assay for reversal of MDR in tumour cells

The cells were adjusted to a density of 2×10^6/mL, resuspended in serum-free McCoy's 5A medium and distributed in 0.5 mL aliquots into Eppendorf centrifuge tubes. 10 μL of test compounds were added at various concentrations (0.025–1 mM), and the samples were incubated for 10 min at room temperature. Next, 10 μL (5.2 mM final concentration) of the indicator rhodamine 123 was added to the samples and the cells were incubated for a further 20 min at 37 °C, washed twice and resuspended in 0.5 mL phosphate-buffered saline (PBS) for analysis. The fluorescence uptake of the cell population was measured with a Beckton Dickinson FACScan flow cytometry. Verapamil was used as a positive control in the rhodamine 123 exclusion experiments. The percentage mean fluorescence intensity was calculated for the treated MDR and parental cell lines as compared to untreated cells. An activity ratio FAR was calculated via the following equation, on the basis of the measured fluorescence values:

$$\text{FAR} = \frac{\text{MDR treated/MDR control}}{\text{Parental treated/parental control}}$$

The results are from a representative flow cytometry experiment in which 10,000 individual cells of the population were investigated; the histograms were evaluated based on the mean fluorescence intensity, standard deviation, peak channel in the total—and in the gated—populations (as an example see flow cytometry data for compound **4** in Supplementary data).

3.4.4. Checkerboard microplate method

The microplate method was applied to study the effects of drug interactions between resistance modifiers and doxorubicin on cancer cells.[34] The effects of the anticancer drug doxorubicin and the resistance modifiers in combination were studied on *MDR1* gene-transfected mouse lymphoma cells. The dilution of doxorubicin (A) was made in a horizontal direction, and the dilutions of resistance modifiers (B) vertically in the microtiter plate, in a volume of 100 μL. The cell suspension in the tissue culture medium was distributed into each well in 100 mL containing 5×10^4 cells. The plates were incubated for 72 h at 37 °C in a CO_2-incubator. The cell growth rate was determined after MTT staining and the intensity of the blue colour was measured on a micro ELISA reader. Drug interactions were evaluated according to the following system:

$FIC_A = ID_{50\ A\ \text{in combination}}/ID_{50\ A\ \text{alone}}$	FIX <0.5 Synergism
$FIC_B = ID_{50\ B\ \text{in combination}}/ID_{50\ B\ \text{alone}}$	FIX = 0.51–1 Additive effect
ID = inhibitory dose	FIX = 1–2 Indifferent effect
FIC = fractional inhibitory concentration	FIX > 2 Antagonism
	FIX = Fractional inhibitory index
	$FIX = FIC_A + FIC_B$

Acknowledgments

The Science and Technology Foundation, Portugal (FCT, grant SFRH/BD/22321/2005) and the Szeged Foundation for Cancer Research supported this work. The authors thank Mrs. Vigyikán Várady Aniko for technical assistance with the tissue cultures, and also Dr. Catarina Arruda and Dr. Guedes de Sousa, from the Portuguese Embassy in Mozambique, as well as the Portuguese Office of International Affairs for plant transport.

Supplementary data

Supplementary data (^1H and ^{13}C NMR spectra of compounds **1**–**3**. Flow cytometry data and energy-minimized 3D structure of compounds for compound **4**) associated with this article can be found, in the online version, at doi:10.1016/j.bmc.2009.08.020.

References and notes

1. Molnár, J.; Gyémánt, N.; Tanaka, M.; Hohmann, J.; Bergmann-Leitner, E.; Molnár, P.; Deli, J.; Didiziapetris, R.; Ferreira, M. J. U. *Curr. Pharm. Des.* **2006**, *12*, 287.
2. Szakács, G.; Paterson, J.; Ludwig, J.; Genthe, C.; Gottesman, M. *Nat. Rev. Drug Disc.* **2006**, *5*, 219.
3. Teodori, E.; Dei, S.; Martelli, C.; Scapecchi, C.; Gualtieri, F. *Curr. Drug Targets* **2006**, *7*, 893.
4. Krishna, R.; Lawrence, D. M. *Eur. J. Pharmaceut. Sci.* **2000**, *11*, 265.
5. Borowski, E.; Bontemps-Gracz, M.; Picokowska, A. *Acta Biochim. Pol.* **2005**, *52*, 609.
6. Szabo, D.; Szabo, G.; Ocsovszki, I.; Aszalos, A.; Molnár, J. *Cancer Lett.* **1999**, *139*, 115.
7. Zalatnai, A.; Molnár, J. *In Vivo* **2006**, *20*, 137.
8. Stouch, T. R.; Gudmundsson, O. *Adv. Drug Delivery Rev.* **2002**, *54*, 315.
9. Seelig, A.; Landwojtowicz, E. *Eur. J. Pharmaceut. Sci.* **2000**, *12*, 31.

10. Srinivas, E.; Murthy, J.; Rao, A.; Sastry, G.. *Curr. Drug Metab.* **2006**, *7*, 205.
11. Flyman, M. V.; Afolayan, A. J. *Int. J. Food Sci. Nutr.* **2007**, *58*, 419.
12. De Tommasi, N.; De Simone, F.; De Feo, V.; Pizza, C. *Planta Med.* **1991**, *57*, 201.
13. De Tommasi, N.; De Simone, F.; Piacente, S. *Nat. Prod. Lett.* **1995**, *6*, 261.
14. Duarte, N.; Járdánházy, A.; Molnár, J.; Hilgeroth, A.; Ferreira, M. J. U. *Bioorg. Med. Chem.* **2008**, *16*, 9323.
15. Duarte, N.; Lage, H.; Ferreira, M. J. U. *Planta Med.* **2008**, *74*, 61.
16. Wesolowska, O.; Wisniewski, J.; Duarte, N.; Ferreira, M. J.; Michalak, K. *Anticancer Res.* **2007**, *27*, 4127.
17. Duarte, N.; Varga, A.; Radics, R.; Molnár, J.; Ferreira, M. J. U. *Bioorg. Med. Chem.* **2007**, *15*, 546.
18. Madureira, A. M.; Gyémant, N.; Ascenso, J. R.; Abreu, P. M.; Molnár, J.; Ferreira, M. J. *J. Nat. Prod.* **2006**, *69*, 950.
19. Ferreira, M. J. U.; Duarte, N.; Gyémánt, N.; Radics, R.; Chepernev, G.; Varga, A.; Molnár, J. *Anticancer Res.* **2006**, *26*, 3541.
20. Duarte, N.; Gyémánt, N.; Abreu, P. M.; Molnár, J.; Ferreira, M. J. U. *Planta Med.* **2006**, *72*, 162.
21. Madureira, A. M.; Spengler, G.; Molnár, A.; Varga, A.; Molnár, J.; Abreu, P. M.; Ferreira, M. J. U. *Anticancer. Res.* **2004**, *24*, 859.
22. Xu, R.; Fazio, G. C.; Matsuda, S. P. T. *Phytochemistry* **2004**, *65*, 261.
23. Takahashi, S.; Satoh, H.; Hongo, Y.; Koshino, H. *J. Org. Chem.* **2007**, *72*, 4578.
24. Fatope, M. O. *J. Nat. Prod.* **1990**, *53*, 1491.
25. Liu, X.; Cui, Y.; Yu, Q.; Yu, B. *Phytochemistry* **2005**, *66*, 1671.
26. Qing-Yan, L.; Hu-Biao, C.; Zhen Ming, L.; Bin, W.; Yu-Ying, Z. *Magn. Reson. Chem.* **2007**, *45*, 451.
27. Nakamura, S.; Murakami, T.; Nakamura, J.; Kobayashi, H.; Matsuda, H.; Yoshikawa, M. *Chem. Pharm. Bull. (Tokyo)* **2006**, *54*, 1545.
28. Cantrell, C. L.; Lu, T.; Fronczek, F. R.; Fischer, H. *J. Nat. Prod.* **1996**, *59*, 1131.
29. Horgen, F. D.; Sakamoto, B.; Scheuer, P. J. *J. Nat. Prod.* **2000**, *63*, 210.
30. Chemical computing Group Inc. MOE v2008.10. 1010 Montreal, Quebec, Canada, 2008.
31. Warren L. DeLano 'The PyMOL Molecular Graphics System'. DeLano Scientific LLC, San Carlos, CA, USA. http://www.pymol.org.
32. Voigt, B.; Coburger, C.; Molnár, J.; Hilgeroth, A. *Bioorg. Med. Chem.* **2007**, *15*, 5110.
33. Cornwell, M. M.; Pastan, I.; Gottesmann, M. M. *J. Biol. Chem.* **1987**, *262*, 2166.
34. Eliopoulos, G. M.; Moellering, R. C. Antimicrobial Combinations. In *Antibiotics in Laboratory Medicine*; Lorian, V., Ed., 3rd ed.; Williams and Wilkins: Baltimore, USA, 1991; pp 434–441.